Inorg. Chem. **2006**, *45*, 3023–3033

Studies of a Dinuclear Manganese Complex with Phenoxo and Bis-acetato Bridging in the Mn_2(II,II) and Mn_2(II,III) States: Coordination Structural Shifts and Oxidation State Control in Bridged Dinuclear Complexes

Yilma Gultneh,*,† Yohannes T. Tesema,†,§ Teshome B. Yisgedu,†,# Ray J. Butcher,† Guangbin Wang,‡ and Gordon T. Yee‡

Departments of Chemistry, Howard University, Washington, D.C. 20059, and Virginia Polytechnic Institute and State University, Blacksburg, Virginia 24061

Received January 8, 2006

The dinucleating ligand, 2,6-bis{[(2-(2-pyridyl)ethyl)(2-pyridylmethyl)-amino]-methyl}-4-methylphenol) (L^1OH) reacts with $Mn(ClO_4)_2 \cdot 6H_2O$ to form the dinuclear complex $[Mn_2(II,II)(L^1O)(\mu\text{-}OOCCH_3)_2]ClO_4$ (**1**). The electrolytic oxidation of **1** at 0.7 V (vs Ag/AgCl) produces the mixed valent complex $[Mn_2(II,III)(L^1O)(\mu\text{-}OOCCH_3)_2](ClO_4)_2$ (**1ox**) quantitatively, while electrolysis at 0.20 V converts **1ox** back to **1**. X-ray crystallographic structures show that both **1** and **1ox** are dinuclear complexes in which the two manganese ions are each in distorted octahedral coordination environments bridged by the phenoxo oxygen and two acetate ions. The structural changes that occur upon the oxidation **1** to **1ox** suggest an extended π-bonding system involving the phenoxo ring $C\text{–}O_{phenoxo}\text{–}Mn(II)\text{–}N_{pyridyl}$ chain. In addition, as **1** is oxidized to **1ox,** the rearrangements in the coordination sphere resulting from the oxidation of one Mn(II) ion to Mn(III) are transmitted via the bridging $Mn\text{–}O_{phenoxo}$ bonds and cause structural changes that render the site of the second manganese ion unfit for the +3 state and hence unstable to reduction. Thus the electrolytic oxidation of **1ox** in acetonitrile at 1.20 V takes up slightly greater than 1 F of charge/mol of **1ox,** but the starting complex, **1ox**, is recovered, showing the instability of the Mn_2(III,III) state that is formed with respect to reduction to **1ox**. Variable-temperature magnetic susceptibility measurements of **1** and **1ox** over the temperature range from 1.8 to 300 K can be modeled with magnetic coupling constants $J = -4.3$ and -4.1 cm^{-1}, respectively showing the weak antiferromagnetic coupling between the two manganese ions in each dinuclear complex, which is commonly observed among similar phenoxo- and bis-1,3-carboxylato-bridged dinuclear Mn_2(II,II) and Mn_2(II,III) complexes.

Introduction

Numerous manganese enzymes, containing dinuclear active sites, that catalyze biological processes[1] are known, such as Mn catalases[1d,2] and arginase.[3] Catalases, which are found in a large variety of cells, catalyze the disproportionation of harmful H_2O_2, a byproduct of O_2 utilization in cells, to H_2O and O_2.[4,5] The crystallographic structures of the bacterial

* To whom correspondence should be addressed. E-mail: ygultneh@howard.edu.

† Howard University.

‡ Virginia Polytechnic Institute and State University.

§ Present address: Department of Chemistry, Duke University, Durham, NC 27708.

Present address: Department of Chemistry, The Ohio State University, Columbus, OH 43210.

(1) (a) Larson, E. J.; Pecoraro, V. L. In *Manganese Redox Enzymes*; Pecoraro, V. L. Ed.; VCH: New York, 1992; p 1. (b) Law, N. A.; Caudle, M. T.; Pecoraro, V. L. *Adv. Inorg. Chem.* **1998**, *46*, 305. (c) Que, L., Jr.; True, A. E.; *Prog. Inorg. Chem.* **1990**, *38*, 97. (d) Dismukes, G. C. *Chem. Rev.* **1996**, *96*, 2909. (e) Weatherburn, D. C. In *Handbook on Metalloproteins*; Bertini, I., Sigel, A., Sigel, H., Eds.; Marcel Dekker: New York, 2001; 193.

(2) (a) Jedrzejas, M. J.; Setlow, P. *Chem. Rev.* **2001**, *101*, 607. (b) Mizobata, T.; Kagawa, M.; Murakoshi, N.; Kusaka, E.; Kameo, K.; Kawata, Y.; Nagai, J. *Eur. J. Biochem.* **2000**, *267*, 4246. (c) Law, N. A.; Caudle, M. T.; Pecoraro, V. L. In *Manganese Redox Enzymes and Model Systems: Properties, Structures and Reactivity*; Pecoraro, V. L., Ed.; Academic Press: San Diego, CA, 1999; Vol. 46. (d) Christianson, D. W. *Prog. Biophys. Mol. Biol.* **1997**, *67*, 217. (d) La Pape, L.; Perret, E.; Michaud-Sorret, I. *J. Biol. Inorg. Chem.* **2002**, *7*, 445. (e) Waldo, G. S.; Fronko, M. M.; Penner-Hahn, J. E. *Biochemistry* **1991**, *30*, 10486.

(3) (a) Ash, D. E.; Cox, J. D.; Christianson, D. W. In *Metal Ions in Biological Systems;* Sigel, A.; Sigel, H., Eds.; Mercel Dekker: New York, 2000; Vol. 37, p 407. (b) Kanyo, Z. F.; Scolnik, L. R.; Ashe, D. E.; Christianson, D. W. *Nature* **1996**, *383*, 554. (c) Reczkowski, R. S.; Ashe, D. E. *J. Am. Chem. Soc.* **1992**, *114*, 10992. (d) Sossong, T. M., Jr.; Khangulov, S. V.; Cavalli, R. C.; Soprano, D. R.; Dismukes, G. C.; Ash, D. E. *J. Biol. Inorg. Chem.* **1997**, *2*, 443.

10.1021/ic060039q CCC: $33.50
Published on Web 03/08/2006

catalases from *Lactobacillus plantarum*[6] and *Thermus thermophilus*,[7] show dinuclear active sites, with a Mn−Mn distance of 3.6 Å, and the manganese ions are coordinated by a histidyl imidazole with at least one bridging carboxylate from glutamate (or aspartate) and H_2O or OH^-.[8] EPR[9] spectroscopic evidence shows a weak antiferromagnetic coupling between manganese ions in the Mn_2(II,II) and Mn_2(II,III) states of the *T. thermophilus* Mn catalase. Although, in the catalytic cycle, these enzymes shuttle between the Mn_2(II,II) and the Mn_2(III,III) states, they have been isolated in four oxidation states ranging from Mn_2(II,II) to Mn_2(III,IV).[10] The mixed-valent states, Mn_2(II,III) and Mn_2(III,IV), of manganese catalase have been shown to be the catalytically inactive forms, therefore minimizing one-electron redox processes is crucial in the mechanism.[11]

Several synthetic dinuclear manganese complexes that mimic catalase activity have been reported[12] some of which show the Mn_2(II,II) ↔ Mn_2(III,III) catalytic cycle of the manganese catalases.[13] Correlating detailed information on the structures and physical and chemical properties of simple synthetic model complexes often provide crucial links that increase the understanding of the structures and catalytic mechanisms of complex metalloenzymes.[14] Dinuclear manganese complexes which incorporate some feature of the manganese catalase active sites include μ-alkoxo-μ-carboxylato,[12g,15] μ-oxo-μ-carboxylato[13d,16] μ-aquo (or μ-hydroxo)-μ-carboxylato,[12e,17] bis-μ-phenoxo,[18] μ-oxo-bis(μ-carboxylato),[19] μ-phenoxo-bis-μ-carboxylato,[20] bis-μ-oxo-μ-carboxylato,[13d,16c,21] bis-μ-alkoxo,[22] bis-μ-oxo, and bis-μ-OH^{-}[23] complexes. Dinuclear manganese complexes of

(4) (a) Khangulov, S. V.; Barynin, V. V.; Voevodskaya, N. V.; Grebenko, A. I. *Biochim. Biophys. Acta* **1990**, *1020*, 305. (b) Kono, Y.; Fridovich, I. *J. Biol. Chem.* **1983**, *25*, 6015. (c) Mizobata, J.; Kagawa, M.; Murakoshi, N.; Kusaka, E.; Kameo, K.; Kawara, Y.; Nagai, J. *Eur. J. Biochem.* **2000**, *267*, 4264. (d) Algood, G. S.; Perry, J. I. *J. Bacteriol.* **1986**, *168*, 563.

(5) (a) Beyer W. F., Jr.; Fridovich, I. In *Basic Life Sciences*; Simic, M. G., Ed.; Plenum: New York, 1988; Vol. 49, p 651. (b) Fronko, R. M.; Penner-Han, J. E.; Bender, C. J. *J. Am. Chem. Soc.* **1988**, *110*, 7554.

(6) Barynin, V. V.; Whittaker, M. M.; Antonyuk, S. V.; Lamzkin, V. S.; Harrison, P. M.; Artymiuk, P. J.; Whittaker, J. W. *Structure* **2001**, *9*, 725.

(7) (a) Antonyuk, S. V.; Mekik-Adamyan, V. R.; Popov, A. N.; Lamzin, V. S.; Hempstead, P. D.; Harrison, P. M.; Artymyuk, P. J.; Barynin, V. V. *Cryst. Rep.* **2000**, *45*, 105. (b) Whittaker, M. M.; Barynin, V. V.; Antonyuk, S. V.; Whittaker, J. W. *Biochemistry* **1999**, *38*, 9126.

(8) (a) Waldo, G. S.; Yu, S.; Penner-Hahn, E. *J. Am. Chem. Soc.* **1992**, *114*, 5869. (b) Waldo, G. S.; Franko, R M.; Penner-Hahn, J. E. *Biochemistry* **1991**, *30*, 10486.

(9) (a) Khangulov, S. V.; Pessiki, P. J.; Barynin, B. V.; Ash, D. E.; Dismukes, G. C. *Biochemistry* **1995**, *34*, 2015. (b) Barynin, V. V.; Hampstead, P. D.; Vagin, A. A.; Antonyuk, S. V.; Mekik-Adamyan, W. R.; Lamzin, V. S.; Harrison, P. M.; Artymiuk, P. J. *J. Inorg. Biochem.* **1997**, *67*, 196 and references therein.

(10) (a) Waldo, G. S.; Penner-Hahn, J. E. *Biochemistry* **1995**, *34*, 1507. (b) Penner-Hahn, J. E. *Structural Properties of the Mn Sites in the Mn Catalases*; Pecoraro, V. L., Ed.; Verlag: New York, 1992; p 29.

(11) (a) Dismukes, G. C. Polynuclear Manganese Enzymes. In *Bioinorganic Catalysis*; Reekijk, J., Ed.; Marcel Dekker: Amsterdam, 1992. (b) Khangulov, S. V.; Barynin, V. V.; Antonyuk-Barynina, S. W. *Biochim. Biophys. Acta* **1990**, *1020*, 25. (c) Khangulov, S. V.; Goldfield, M. G.; Gerasimenko, V. V.; Andreeva, N. E.; Barynin, V. V.; Grebenko, A. I. *J. Inorg. Biochem.* **1990**, *40*, 279. (d) Michaud-Soret, I.; Jacquamet, L.; Debaecker-Petit, N.; Le Pape, L.; Barynin, V. V.; Latour, J. M. *Inorg. Chem.* **1998**, *37*, 3674.

(12) (a) For a recent comprehensive review, see: Wu, A. J.; Penner-Hahn, J. E.; Pecoraro, V. L. *Chem. Rev.* **2004**, *104*, 903. (b) Gelasco, A.; Askenas, A.; Pecoraro, V. L. *Inorg. Chem.* **1996**, *35*, 1419. (c) Gelasco, A.; Kirk, M. L.; Kampf, J. W.; Pecoraro, V. L. *Inorg. Chem.* **1997**, *36*, 1829. (d) Sakiyama, H.; Okawa, H.; Isobe, R. *J. Chem. Soc., Chem. Commun.* **1993**, 882. (e) Bolreijk, A. E. M.; Dismukes, G. C. *Inorg. Chem.* **2000**, *39*, 3020. **(f)** Dubois, L.; Caspar, R.; Jacquamet, L.; Petit, P.-E.; Charlot, M.-F.; Baffert, C.; Collomb, M.-N.; Deronzier, A.; Latour, J.-M. *Inorg. Chem.* **2003**, *42*, 4817. (g) Palopoli, C.; Gonzalez-Sierra, M.; Robles, G.; Dahan, F.; Tuchagues, J.-P.; Signorella, S. *J. Chem. Soc., Dalton Trans.* **2002**, 3813. (h) Buchanan, R. M.; Oberhausen, K. J.; Richardson, J. F. *Inorg. Chem.* **1988**, *27*, 971. (i) Itoh, M.; Motoda, K.; Kamiusuli, T.; Sakiyama, H.; Matsumo, N.; Okawa, H. *J. Chem. Soc., Dalton Trans.* **1995**, 3635. (j) Doctrow, S. R.; Huffman, K.; Marcus, C. B.; Tocco, G.; Malfroy, E.; Adinolfi, C. A.; Kruk, H.; Baker, K.; Lazarowych, N.; Mascarenhas, J.; Malfroy, B. *J. Med. Chem.* **2002**, *45*, 4549.

(13) (a) Pecoraro, V. L.; Baldwin, M. J.; Gelasco, A. *Chem. Rev.* **1994**, *94*, 807. (b) Boelrijk, A. E. M.; Khangulov, S. V.; Dismukes, G. C. *Inorg. Chem.* **2000**, *39*, 3009. (c) Gelasco, A.; Pecoraro, V. L. *J. Am. Chem. Soc.* **1993**, *115*, 7928. (d) Mukopadhyay, S.; Staples, J.; Armstrong, W. H. *J. Chem. Soc. Chem. Commun.* **2002**, 864. (e) Dubé, C. E.; Wright, D. W.; Armstrong, W. H. *Angew. Chem., Int. Ed. Engl.* **2000**, *39*, 2169. (f) Tanase, T.; Lippard, S. J. *Inorg. Chem.* **1995**, *34*, 4682.

(14) (a) Pecoraro, V. L.; Gelasco, A.; Baldwin, M. J. In *Modeling the Chemistry and Properties of Multinuclear Centers*; Kessissoglou, D. P., Ed.; Kluwer Academic Publishers: Dodrecht,The Netherlands, 1995; p 287. (b) Peloquin, J. M.; Campbell, K. A.; Randall, D. W.; Evanchik, V. L.; Pecoraro, V. L.; Armstrong, W. H.; Britt, R. D. *J. Am. Chem. Soc*. **2000**, *122*, 10926. (c) Dunand-Sauthier, M.-N. C.; Deronzier, A.; Piron, A.; Pradon, X.; Menage, S. *J. Am. Chem. Soc.* **1998**, *120*, 5373.

(15) (a) Pessiki, P. J.; Khangulov, S. V.; Vo, D. M.; Dismukes, G. C. *J. Am. Chem. Soc*. **1994**, *116*, 891. (b) Pessiki, P. J.; Dismukes, G. C. *J. Am. Chem. Soc.* **1994**, *116*, 898. (c) Bertoncello, K.; Fallon, G. D.; Murray, K. S. *Polyhedron* **1990**, *9*, 2867. (d) Daier, V.; Biava, H.; Palopoli, C.; Shova, S.; Tuchagues, J.-P.; Signorella, S. *J. Inorg. Biochem.* **2004**, *98*, 1806.

(16) (a) Oberhausen, K. J.; O'Brien, R. J.; Richardson, J. F.; Buchanan, R. M.; Cost, R.; Latour, J.-M.; Tsai, H.-L.; Hendrickson, D. N. *Inorg. Chem*. **1993**, *32*, 4561. (b) Brundenell, S. J.; Spiccia, L.; Bond, A. M.; Fallon, G. D.; Hockless, D. C. R.; Lazarev, G.; Mahon, P. J.; Tiekink, E. T. R. *Inorg. Chem.* **2000**, *39*, 881. (c) Osawa, M.; Fujisawa, K.; Kitajima, N.; Moro-oka, Y. *Chem. Lett.* **1997**, *26*, 919. (d) Arulsamy, N.; Glerup, J.; Hazell, A.; Hodges, D. J.; McKenzie, C. J.; Toflund, H. *Inorg. Chem.* **1994**, *33*, 3023.

(17) (a) Coucouvanis, D.; Reynolds, R. A, III; Dunham, W. R. *J. Am. Chem. Soc*. **1995**, *117*, 7570. (b) Ye, B. H.; Mak, T.; Williams, I. D.; Li, X. Y. *J. Chem. Soc., Chem. Commun.* **1997**, 1813. (c) Yu, S. B.; Lippard, S. J.; Shweky, I.; Bino, A. *Inorg. Chem.* **1992**, *31*, 3502. (d) Xiang, D. F.; Tan, X. S.; Tang, W. S.; Xue, F.; Mak, T. C. W. *Polyhedron* **1998**, *17*, 1375.

(18) (a) Vincent, J. B.; Folting, K.; Huffman, J. C.; Christou, G. *Inorg. Chem*. **1986**, *25*, 996. (b) Downard, A. J.; McKee, V.; Tandon, S. *Inorg. Chim. Acta* **1990**, *173*, 181. (c) Koizumi, S.; Nehei, M.; Oshio, H. *Chem. Lett*. **2004**, *33*, 896. (d) Yu, S.-B.; Wang, C.-P.; Day, E. P.; Holm, R. H. *Inorg. Chem.* **1991**, *30*, 4067. (e) Reddig, N.; Pursche, D.; Kloskowski, M.; Slinn, C.; Baldeau, S. M.; Rompel, A. *Eur. J. Inorg. Chem.* **2004**, 879.

(19) (a) Gultneh, Y.; Ahvazi, B.; Khan, A. R.; Butcher, R. J.; Tuchagues, J. P. *Inorg. Chem.* **1995**, *34*, 3633. (b) Wu, F.-J.; Kurtz, D. M. Jr.; Hagen, K. S.; Nyman, P. D.; Debrunner, P. G.; Vankai, V. S. *Inorg. Chem*. **1990**, *29*, 5174. (c) Wieghardt, K.; Bossek, U.; Bonvoisin, J.; Beauvillain, P.; Girerd, J. J.; Nuber, B.; Weiss, J.; Heinze, J. *Angew. Chem., Int. Ed. Engl*. **1986**, *25*, 1030. (d) Mahapatra, S.; Lal, T. K.; Mukherjee, R. *Inorg. Chem*. **1994**, *33*, 1579. (f) Mandal, S. K.; Armstrong, W. H. *Inorg. Chim. Acta* **1995**, *229*, 261.

(20) (a) Gultneh, Y.; Farooq, A.; Liu, S.; Karlin, K. D.; Zubieta, J. *Inorg. Chem.* **1992**, *31*, 3607. (b) Diril, H.; Chang, H.-R.; Nilges, M. J.; Zhang, X.; Potenza, J. A.; Schugar, H. J.; Isied, S. S.; Hendrickson, D. N. *J. Am. Chem. Soc*. **1989**, *111*, 5102. (c) Diril, H.; Chang, H.-R.; Zhang, X.; Larsen, S. K.; Potenza, J. A.; Pierpont, C. G.; Isied, S. S.; Hendrickson, D. N. *J. Am. Chem. Soc.* **1987**, *107*, 6207. (d) Chang, H. R.; Diril, H.; Nilges, M. J.; Zhang, X.; Potenza, J. A.; Schugar, H. J.; Hendrickson, D. N.; Isied, S. S. *J. Am. Chem. Soc.* **1988**, *110*, 625. (e) Suzuki, M.; Murata, S.; Uehara, A.; Kida, S. *Chem. Lett*. **1987**, 281.

(21) (a) Torayama, H.; Nishidi, T.; Asada, H.; Fujiwara, M.; Matsushita, T. *Polyhedron* **1998**, *17*, 105. (b) Lal, T. K.; Mukherjee, R. *Inorg. Chem.* **1998**, *37*, 2373. (c) Romero, I.; Dubois, L.; Collomb, M.-N.; Deronzier, A.; Latour, J.-M.; Pécault, J. *Inorg. Chem*. **2002**, *41*, 1795.

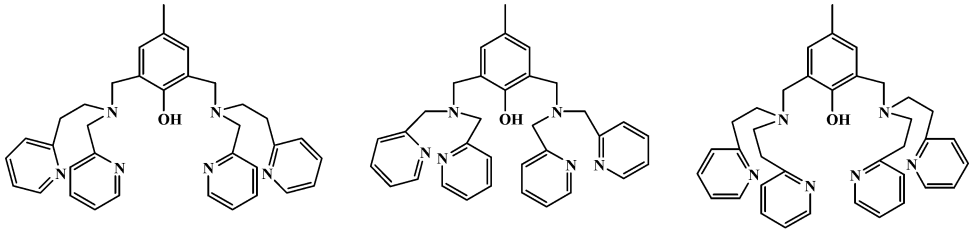

L^1OH L^2OH L^3OH

Figure 1. Structures of the dinucleating ligands L^1OH, L^2OH, and L^3OH.

tridentate ligands bearing facially capped N-donor groups, such as bis(2-pyridylmethyl)amine (bpa),[19a,24] bis-2-(2-pyridylmethyl)ethylamine (bpea),[23a] and (2-pyridylmethyl)(2-(2-pyridyl)ethyl) methylamine,[25] are known in various oxidation states. Reports of model complexes in the mixed-valent Mn_2(II,III) state are fewer[26] than those in the Mn_2(II,II) state.

The dinucleating ligands, 2,6-bis[bis(2-pyridylmethyl)-aminomethyl]-4-methyl phenol)(L^2OH) and 2,6-bis[(bis(2-(2-pyridyl)ethyl)-aminomethyl)-4-methylphenol(L^3OH) (Figure 1), which differ only in their chelate arm lengths, yield phenoxo oxygen- and bis-1,3-carboxylato-bridged dinuclear manganese complexes with two five-membered (5,5) and two six-membered (6,6) chelate rings, respectively. While L^2-OH yields $[Mn_2(II,II)(L^2O)(OAc)_2](ClO_4)$ (**2**)[27] and $[Mn_2$-(II, III)$(L^2O)(OAc)_2](ClO_4)_2$ (**2ox**)[20] in stable forms, L^3OH yields only $[Mn_2(II,II)(L^3O)(1,3\text{-}\mu\text{-}OAc)_2](ClO_4)$ (**3**)[28] in a stable form. In their cyclic voltamograms, **2** shows quasi-reversible Mn(II,II) ↔ Mn(II, III) and Mn(II, III) ↔ Mn-(III, III) redox processes, whereas **3** shows a quasi-reversible Mn(II,II) ↔ Mn(II,III) process and an irreversible Mn(II,-III) to Mn(III,III) oxidation; for each process, **3** shows higher potentials than **2**. L^1OH forms analogous manganese complexes exhibiting mixed five and six-membered chelate rings (5,6) at each manganese ion. A study of the structures and stabilities of the oxidation states of the dinuclear manganese complexes of this ligand, combined with those of L^2OH and L^3OH, reveal some of the chemical implications of ligand-imposed bond angles and lengths in these complexes and the relevance of this to the active sites of metalloenzymes.

We report here the synthesis and structural, spectroscopic, electrochemical, and magnetic properties of the dinuclear manganese complexes of L^1OH, $[Mn_2(II,II)(L^1O)(OAc)_2]$ (ClO_4) (**1**) and $[Mn_2(II,III)(L^1O)(OAc)_2]$ $(ClO_4)_2$ (**1ox**). A comparison is made of the structural parameters of these two complexes with those of the analogous complexes of L^2OH (**2** and **2ox**) and L^3OH (**3**), and correlations are made with their voltammetric potentials, electronic absorption spectra, and magnetic properties. The structural changes that occur upon oxidation of **1** to **1ox** and **2** to **2ox** explain why the Mn_2(III,III) states of these sets of ligands are unstable with respect to reduction.

These instabilities are rationalized on the basis of the differences in the coordination geometry and radii preferences of Mn(II) and Mn(III) ions and those provided by the ligands. Control of the metal coordination geometry and radii in metalloenzymes is thought[29] to be a possible mechanism for the switching on or off of certain oxidation states and hence catalysis. The highly efficient dismutation of H_2O_2 by manganese catalases requires simultaneous two-electron redox cycles, made possible by electronic decoupling of the two metal ions to avoid one-electron redox processes.[1d] The study presented here illustrates the effects of ligand-imposed bond angles and lengths and dynamic structural shifts that dictate one-electron redox processes and limit the stability of the oxidation states in dinuclear metal complexes and these results could be relevant to enzyme mechanisms.

Experimental Section

Materials and Techniques. 2-Picolyl chloride hydrochloride, KBr, KOH, sodium acetate, $Mn(ClO_4)_2 \cdot 6H_2O$, NaOH, 2-hydroxy-5-methyl-1,3-benzenedicarboxaldehyde, and vinyl-2-pyridine were all reagent grade and were used as received from Aldrich Chemical Co. The solvents used were all reagent grade, further purified by refluxing over drying agents and distilling under a nitrogen atmosphere. Ether was distilled from Na/benzophenone; acetonitrile was predried over P_4O_{10} and distilled from CaH_2, and methanol

(22) (a) Gelasco, A.; Bensiek, S.; Pecoraro, V. L. *Inorg. Chem*. **1998**, *37*, 3301. (b) Gelasco, A.; Kirk, M. L.; Kampf, J. W.; Pecoraro, V. L. *Inorg. Chem.* **1997**, *36*, 1829. (c) Mikuriya, M.; Yamato, Y.; Tokii, T. *Bull. Chem. Soc. Jpn.* **1992**, *65*, 2624.

(23) (a) Gultneh, Y.; Yisgedu, T. B.; Tesema, Y. T.; Butcher, R. J. *Inorg. Chem.* **2003**, *42*, 1857. (b) Triller, M. U.; Hsieh, W.-Y., Pecoraro, V. L.; Rompel, A.; Krebs, B. *Inorg. Chem.* **2002**, *41*, 5544. (c) Kitajima, N.; Singh, U.; Amagai, H.; Osawa, M.; Moro-Oka, Y. *J. Am. Chem. Soc.* **1991**, *113*, 7757.

(24) Drechsel, S. M.; Mangrich, A. S.; Budel, M. V.; Tavares, F. Abstracts, Eighth International Conference on Bioinorganic Chemistry. *J. Inorg. Biochem*. **1997**, *67*, 202. (c) Wu, J.-Z.; Bouwman, E.; Mills, A. M.; Spek, A. L.; Reedijk, J. *Inorg. Chim. Acta* **2004**, *357*, 2694.

(25) (a)Mahapatra, S.; Das, P.; Mukherjee, R. N. *Chem. Soc. Dalton Trans*. **1993**, 217. (b) Gupta, N.; Mukerjee, S.; Mahapatra, S.; Ray, M.; Mukherjee, R. N. *Inorg. Chem.* **1992**, *31*, 139.

(26) (a) Dubois, L.; Xiang, D.-F.; Tan, S.-S.; Pecaut, J.; Jones, P.; Baudron, S.; Le Pape, L.; Latour, J.-M.; Baffer, C.; Chardon-Noblat, S.; Collomb, M.-N.; Deronzier, A. *Inorg. Chem.* **2003**, *42*, 750. (b) Suzuki, M.; Mikuriya, M.; Murata, S.; Uehara, A.; Oshio, H.; Kida, S.; Saito, K. *Bull. Chem. Soc. Jpn.* **1987**, *60*, 4305. (c) Karsten, P.; Neves, A.; Bortoluzzi, A.; Strhle, J.; Maichle-Mossmer, C. *Inorg. Chem. Commun.* **2002**, *5*, 434. (d) Mikuriya, M.; Fujii, T.; Tokii, T.; Kawamori, A. *Bull. Chem. Soc. Jpn.* **1993**, *66*, 1675.

(27) Blanchard, S.; Blondin, G.; Riviere, E.; Nierlich, M.; Girerd, J.-J. *Inorg. Chem.* **2003**, *42*, 4568 (note that the value of $J = -9.6$ cm^{-1} was arrived at in this reference using the Hamiltonian $H = -JS_1S_2$, while those in the present work were calculated using $H = -2JS_1S_2$, so that for comparison purposes we have used J = half of -9.6 cm^{-1} $= -4.8$ cm^{-1}).

(28) A study of the structure and redox properties of **3** has been separately submitted for publication. The redox potentials are given in Table 6.

(29) (a) Messerschmidt, A.; Prade, L.; Kroes, S. J.; Sanders-Loehr, J.; Huber, R.; Canters, G. W. *Proc. Natl. Acad. Sci. U.S.A.* **1998**, *95*, 3443. (b) van Amsterdam, I. M. C.; Ubbink, M.; van den Bosch, M.; Rotsaert, F.; Sanders-Loehr, J.; Canters, G. W. *J. Biol. Chem.* **2002**, *277*, 44121.

Scheme 1. Synthesis of the Ligand L^1OH

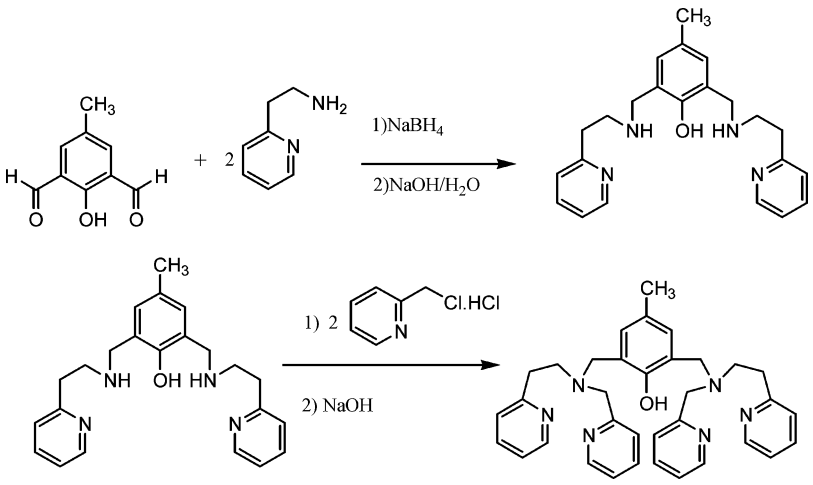

was distilled from $Mg(OCH_3)_2$. Vinyl pyridine (Aldrich) was vacuum distilled just before use. The synthesis of the Mn(II) complex was performed under argon using vacuum/inert gas-line and airless-glassware techniques. Elemental analyses were performed by Desert Analytics (Tucson, AZ). ^{1}H NMR spectra were taken in solution in deuterated solvents with an internal TMS standard on a GE 300 MHz spectrometer. IR spectra were taken on a Nicolet 560 FT-IR spectrophotometer on samples as KBr mulls. Electronic spectra were taken using a Hewlett-Packard HP 8453 diode-array spectrophotometer, in acetonitrile solutions, using a 1.0 cm quartz cuvette.

Cyclic voltammetric measurements were done using a BAS 100B electrochemical analyzer on 2.0 mM solutions of metal complexes in dried and degassed acetonitrile containing 0.1 M tetra-*n*-butylammonium perchlorate (TBAP) as the supporting electrolyte. The solutions were sparged with predried nitrogen gas for 10 min prior to each scan and blanketed with nitrogen during each scan. A glassy carbon working electrode, a platinum wire counter electrode, and an Ag/AgCl reference electrode were used.

Controlled potential and bulk electrolytic oxidation and reduction experiments were also performed on a BAS 100B electrochemical analyzer. The cell consisted of a platinum wire mesh basket working electrode, Ag/AgCl reference electrode with the complex dissolved in acetonitrile with 0.1 M $NaClO_4$ as the supporting electrolyte. A platinum wire auxiliary electrode is dipped in 0.1 M $NaClO_4$ dissolved in CH_3CN in a sidearm compartment separated by glass frit. A Fisher conductivity/pH meter apparatus with a YSI conductance cell (0.1 cm) was used for measuring the molar conductance of 1.0 mM solutions of the complexes in acetonitrile.

X-ray Crystallographic Structure Determination. A suitable crystal of the complex was mounted in a random orientation on the end of a glass fiber using 5 min epoxy cement and transferred to a goniometer head. All measurements were made on a Bruker SMART 1K CCD four-circle X-ray diffractometer using Mo Kα radiation of wavelength 0.71069 Å equipped with a graphite monochromator on the incident beam. The space group was unambiguously obtained from a statistical examination of the intensities of the collected data set. The structure was solved by direct methods as implemented in the SHELXTL system of computer programs.[30] The structure was refined to convergence using full-matrix least-squares methods. The hydrogen atoms were included in their idealized positions. One arm of the ligand of **1** was disordered over two conformations with occupancies of 0.610 and 0.390.[31] All diagrams include only the major conformation.

Magnetic Measurements. All the magnetic measurements were performed on a 7 T Quantum Design MPMS SQUID magnetometer. Roughly 15 mg of microcrystal samples were sandwiched between cotton plugs and placed into gel capsules. Measurements of magnetization as a function of temperature were performed from 1.8 to 300 K in an applied field of 1000 G. Samples were cooled in zero field and measured upon warming. Diamagnetic corrections were applied based on Pascal's constants.[32]

Synthesis of Ligands and Complexes. ***Caution:*** *Although we have not encountered any incidents in the work described in this paper, perchlorates combined with organic compounds are potentially explosive and should be used in small quantities and with caution.*

The synthetic route used in making L^1OH is shown in Scheme 1.

2,6-Bis[(2-(2-pyridyl)ethylamino)-methyl]-4-methyl-phenol. 2-(2-Aminoethyl)-pyridine[33] (1.5 g, 12.2 mmol) dissolved in 10 mL of freshly distilled methanol was added, dropwise, to a solution of 2-hydroxy-5-methyl-1,3-benzenedicarboxaldehyde (1.0 g, 6.09 mmol) in 10 mL of methanol. After the mixture was stirred for 3 h, a solution of sodium borohydride (0.92 g, 24.4 mmol) in 20 mL of water containing sodium hydroxide (0.4 g, 10 mmol) was added dropwise. The resulting light pink solution was stirred for 3 h and concentrated under reduced pressure; the residue was then extracted with three 25 mL portions of chloroform. The combined extract was dried over anhydrous $MgSO_4$ and filtered, and the solvent was removed under reduced pressure to yield a yellow oil (2.1 g, 93% yield). ^{1}H NMR ($CDCl_3$−TMS): δ 2.17 (s, 3H), 3.00 (m, 8H), 3.85 (s, 4H), 6.78 (s, 2H), 7.12 (m, 4H), 7.56 (t, 2H), 8.49 (d, 2H).

2,6-Bis{(2-(2-pyridyl)ethyl)(2-pyridylmethyl)aminomethyl}4-methylphenol (L^1OH). A solution of 2-picolyl chloride hydrochloride (2.8 g, 17.07 mmol) in 20 mL of water was cooled to 0 °C in an ice bath and neutralized by dropwise addition of an ice-cooled aqueous 2 M solution of NaOH (9 mL). To this solution was added, with vigorous stirring, a solution of 2,6-bis[(2-(2-pyridyl)ethyl)amino)-methyl]-4-methylphenol (3.21 g, 8.53 mmol)

(30) Sheldrick, G. M. *SHELXTL*, version 5.10; Bruker AXS Inc.: Madison WI, 1997.

(31) In the cation of **1**, $[Mn_2(L^1O)(\mu\text{-}OOCCH_3)_2]^+$, the arm of the ligand attached to Mn(2) is disordered over two conformations with occupancies of 0.692(5) and 0.308(5). Thus some of these differences in the coordination sphere about Mn(2) may be caused by this disorder. All tables include only parameters from the major conformation. The supplementary data contain the complete list of all parameters.

(32) Khan, O. *Molecular Magnetism*; VCH: New York 1993.

in 25 mL of CH_2Cl_2, which had been cooled in an ice bath prior to the addition. The mixture was stirred at 0 °C for 6 h, and then it was allowed to warm to room temperature and was stirred for another 6 h; the pH was maintained at 9−10 by the dropwise addition of a 10% NaOH solution. The reaction mixture was extracted with three 25 mL portions of CH_2Cl_2. The combined extract was dried over anhydrous $MgSO_4$. The solution was filtered and evaporated under reduced pressure, and the desired product was obtained as brown oil (3.69 g, 77.5% yield). ^{1}H NMR ($CDCl_3$−TMS): δ 2.24 (s, 3H), 3.18 (m, 4H), 3.33 (t, 4H), 3.47 (s, 4H), 4.13 (s, 2H), 4.23 (2, 2H), 4.67 (s, H), 7.14 (m, 6H), 7.57 (m, 6H), 8.39 (d, 2H), 8.48 (d, 2H).

$[Mn_2(L^1O)(\mu\text{-}OAC)_2]ClO_4$ (1). A solution of the ligand L^1OH (0.89 g, 1.59 mmol), triethylamine (0.2 g, 1.9 mmol), and CH_3-COONa (0.52 g, 6.37 mmol) in methanol (15 mL) was added to a solution of $Mn(ClO_4)_2 \cdot 6H_2O$ (1.15 g, 3.19 mmol) in methanol (10 mL) under argon, and the mixture was stirred. After 3 to 5 min, a colorless powdery precipitate formed which was filtered, washed with 20 mL of a methanol/ether (1/1) mixture, and then washed with 20 mL of ether. The powder was dried under vacuum to yield 1.0 g (71% yield) of the complex. Crystals suitable for X-ray crystallography were obtained from a CH_3CN solution layered with dry ether. Anal. Calcd for $C_{39}H_{43}ClMn_2N_6O_9$: C, 52.92; H, 4.99; N, 9.49. Found: C, 53.38; H, 5.44; N, 8.96. IR spectrum (KBr disk): 1603 (pyridyl ring), 1420, 1580 (bridging acetate), 1180 cm^{-1} (ClO_4^-). UV−vis absorption spectrum in CH_3CN: λ_{max} (ϵ) 257 (1.36×10^4), 311 nm (3.55×10^3 M^{-1} cm^{-1}).

Electrochemical Synthesis of $[Mn_2(L^1O)(OAC)_2](ClO_4)_2$ (1ox). A platinum mesh basket working electrode and a Ag/AgCl reference electrode were dipped in a 0.1 M $NaClO_4$ supporting electrolyte solution in acetonitrile (25 mL) in which 0.46 g (5.2×10^{-5} mol) of **1** has been dissolved. A platinum wire auxiliary electrode was placed in a sidearm compartment separated by glass frit, containing 10 mL of 0.1 M $NaClO_4$ in CH_3CN. Electrolysis was performed at a controlled potential of 0.7 V (vs Ag/AgCl) for 1 h. Completion of the bulk electrolysis was assumed when the final current was less than 5% of the initial current. The green solution obtained was vacuum evaporated to remove the solvent, and the residue was extracted with CH_2Cl_2 to give a green solution leaving behind the supporting electrolyte. After filtration and evaporation of the CH_2-Cl_2 solution, a powdery green solid was obtained. Crystals suitable for X-ray diffraction crystallography were obtained by dissolving the green powder in CH_2Cl_2 and layering with dry ether. Anal. Calcd for $C_{39}H_{43}Cl_2Mn_2N_6O_{13}$: C, 47.60; H, 4.38; N, 8.56; Found: C, 47.62; H, 4.70; N, 8.22.

Results and Discussion:

Crystal Structure of $[Mn_2L^1O\text{-}(\mu\text{-}OAc)_2](ClO_4)$ (1). The crystal data and refinement parameters for **1** are shown in Table 1. Table 2 shows selected bond lengths and angles. Figure 2 shows an ORTEP representation of the cation of **1**, $[Mn_2(L^1O)(\mu\text{-}OAc)_2]^+$, with the atom labels. Complex **1** is a dinuclear Mn(II) complex in which each Mn(II) ion is coordinated in a distorted octahedral geometry by the tertiary amine nitrogen (N_{am}),[34] two pyridyl nitrogens (N_{py}), a bridging phenoxo oxygen (O_{ph}), and one oxygen each from two 1,3-bridging acetate ions (O_{ac}).[31]

The three nitrogens of each of the two chelating arms of the ligand (L^1O^-) coordinate facially forming one five- and one six-membered chelate ring. The nitrogen of the longer 2-(2-pyridyl)ethyl arm coordinates trans to the phenoxo oxygen (O_{ph}) at each Mn(II). The Mn−N_{am} bonds are both longer than Mn−N_{py} bonds which is usual in this type of complex.[13d,26a,35] The two manganese ions, Mn(1) and Mn-(2), in the dinuclear unit show significant differences in their bond lengths and angles.[31] Thus, the bite angle of the six-membered chelate rings are 80.11(9)° at Mn(1) and 85.1-(2)° at Mn(2), and the O_{ph}−Mn−N trans angles are 165.52-(9)° for Mn(1) and 172.72(12)° for Mn(2). The bridging acetates are staggered relative to each other, each acetate coordinating to the two manganese ions asymmetrically, as

Table 1. Crystal Data and Structure Refinement for Complex **1** and **1ox**

	1	**1ox**
formula	$C_{39}H_{43}ClMn_2N_6O_9$	$C_{40}H_{45}Cl_4\ Mn_2N_6O_{13}$
fw	885.12	1069.5
temp	93 (2) K	103(2) K
λ.	0.71073 Å	0.71073 Å
cryst syst.	monoclinic	triclinic
space group	$P2_1/n$	$P\bar{1}$
unit cell	a = 16.0118 (15) Å	a = 11.16(3) Å
	b = 15.5369 (14) Å	b = 14.20 (5) Å
	c = 17.9705 (17) Å	c = 16.46 (6) Å
	α = 90°	α = 106.08(8)°
	β = 103.595(2)°	β = 96.19(8)°
	γ = 90°	γ = 95.71(8)°
vol, Z	4345.3(7) Å^3, 4	2469(14) Å^3, 2
density (calcd)	1.353 Mg/m^3	1.439 Mg/m^3
abs coeff	0.700 mm^{-1}	0.792 mm^{-1}
GOF on F^2	1.051	0.924
Final R Indices [$I > 2\sigma(I)$]	R1 = 0.0614,	R1 = 0.0428
	wR2 = 0.1620	wR2 = 0.1069
R indices (all data)	R1 = 0.0886,	R1 = 0.0687
	wR2 = 0.1786	wR2 = 0.1135

Table 2. Selected Bond Lengths (Å) and Angles (deg) of **1**

Mn(1)−O(1A)	2.126(2)	Mn(1)−O	2.134(2)
Mn(1)−O(1B)	2.140(2)	Mn(1)−N(1B)	2.298(3)
Mn(1)−N(1)	2.301(3)	Mn(1)−N(1A)	2.352(3)
Mn(2)−O	2.113(2)	Mn(2)−O(2B)	2.133(2)
Mn(2)−O(2A)	2.160(3)	Mn(2)−N(2B)	2.194(16)
Mn(2)−N(1C)	2.300(3)	Mn(2)−N(1D)	2.308(3)
Mn(2)−N(2A)	2.361(6)	Mn(1)−Mn(2)	3.469(2)

O(1A)−Mn(1)−O	98.29(9)	O(1A)−Mn(1)−O(1B)	99.00(9)
O−Mn(1)−O(1B)	92.68(8)	O(1A)−Mn(1)−N(1B)	91.33(10)
O−Mn(1)−N(1B)	165.50(9)	O(1B)−Mn(1)−N(1B)	96.52(9)
O(1A)−Mn(1)−N(1)	89.75(9)	O−Mn(1)−N(1)	87.25(9)
O(1B)−Mn(1)−N(1)	171.17(9)	N(1B)−Mn(1)−N(1)	81.95(10)
O(1A)−Mn(1)−N(1A)	163.43(10)	O−Mn(1)−N(1A)	87.78(8)
O(1B)−Mn(1)−N(1A)	96.09(9)	N(1B)−Mn(1)−N(1A)	80.14(9)
N(1)−Mn(1)−N(1A)	75.08(9)	O−Mn(2)−O(2B)	95.38(8)
O−Mn(2)−O(2A)	92.00(9)	O(2B)−Mn(2)−O(2A)	100.83(1)
O−Mn(2)−N(1C)	100.27(9)	O(2B)−Mn(2)−N(1C)	89.16(11)
O(2A)−Mn(2)−N(1C)	163.42(10)	O−Mn(2)−N(1D)	170.42(10)
O(2B)−Mn(2)−N(1D)	92.14(10)	O(2A)−Mn(2)−N(1D)	80.73(11)
N(1C)−Mn(2)−N(1D)	85.75(11)	O−Mn(2)−N(2A)	86.33(14)
O(2B)−Mn(2)−N(2A)	163.45(14)	O(2A)−Mn(2)−N(2A)	95.55(14)
N(1C)−Mn(2)−N(2A)	74.35(15)	N(1D)−Mn(2)−N(2A)	88.15(15)
Mn(2)−O−Mn(1)	109.54(9)	C(5)−O−Mn(2)	128.26(18)
C(5)−O−Mn(1)	120.44(17)		

(33) (a) Nelson, S. M.; Rodgers, J. *Inorg. Chem.* **1967**, *6*, 1390. (b) Romary, J. K.; Zechariasen, J. K.; Barger, H. D.; Schiesser, H. J. *J. Chem. Soc. Chem. Commun*. **1968**, 2884.

(34) Abbreviatin used in the paper are as follows: N_{am} = tertiary amine nitrogen, N_{py} = pyridyl nitrogen, O_{ph} = phenoxo oxygen, C_{ph} = phenyl carbon bonded to the phenoxo oxygen, $N_{py,tr}$ = pyridyl nitrogen coordinated trans to the phenoxo oxygen; $N_{py,\ cis}$ = pyridyl nitrogen coordinated cis to the phenoxo oxygen, and O_{ac} = acetate oxygen.

(35) Ikura, H.; Nagata, T. *Inorg. Chem.* **1998**, *37*, 4702.

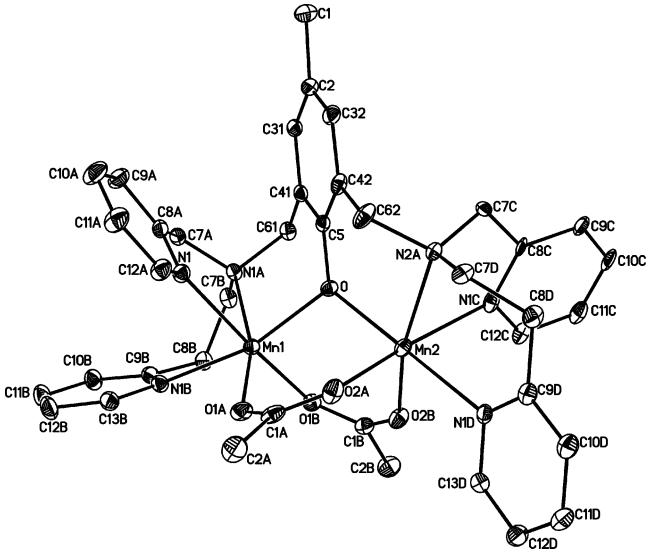

Figure 2. ORTEP diagram showing the 20% probability ellipsoids of the positions of the atoms in the cation of **1**.

Table 3. Selected Bond Lengths (Å) and Angles (deg) of **1ox**

Mn(1)−O	1.891(5)	Mn(2)−N(1C)	2.228(6)
Mn(1)−O(21)	1.923(5)	Mn(2)−O	2.237(6)
Mn(1)−N(1B)	2.035(7)	Mn(2)−N(1D)	2.247(5)
Mn(1)−N(1)	2.065(5)	Mn(2)−N(2)	2.341(5)
Mn(1)−O(11)	2.151(6)	O−C(1)	1.376(4)
Mn(1)−N(1A)	2.290(7)	Mn(1)−Mn(2)	3.486(6)
Mn(2)−O(12)	2.106(6)		
Mn(2)−O(22)	2.112(5)		

O−Mn(1)−O(21)	97.52(14)	O(11)−Mn(1)−N(1A)	174.17(7)
O−Mn(1)−N(1B)	174.17(8)	O(12)−Mn(2)−O(22)	94.9(3)
O(21)−Mn(1)−N(1B)	88.13(14)	O(12)−Mn(2)−N(1C)	94.91(19)
O−Mn(1)−N(1)	94.15(16)	O(22)−Mn(2)−N(1C)	95.1(2)
O(21)−Mn(1)−N(1)	168.02(9)	O(12)−Mn(2)−O	97.06(19)
N(1B)−Mn(1)−N(1)	80.28(16)	O(22)−Mn(2)−O	86.3(2)
O−Mn(1)−O(11)	92.92(18)	N(1C)−Mn(2)−O	167.78(7)
O(21)−Mn(1)−O(11)	93.0(3)	O(12)−Mn(2)−N(1D)	91.3(3)
N(1B)−Mn(1)−O(11)	85.31(19)	O(22)−Mn(2)−N(1D)	172.25(8)
N(1)−Mn(1)−O(11)	89.1(3)	N(1C)−Mn(2)−N(1D)	89.1(2)
O−Mn(1)−N(1A)	92.78(19)	O−Mn(2)−N(1D)	88.2(2)
O(21)−Mn(1)−N(1A)	87.4(2)	O(12)−Mn(2)−N(2)	166.08(8)
N(1B)−Mn(1)−N(1A)	88.9(2)	O(22)−Mn(2)−N(2)	98.8(3)
N(1)−Mn(1)−N(1A)	89.3(3)	N(1C)−Mn(2)−N(2)	81.4(2)
O−Mn(2)−N(2)	86.4(2)		
C(1)−O−Mn(1)	126.40(16)		
C(1)−O−Mn(2)	114.7(3)		
Mn(1)−O−Mn(2)	115.0(2)		

shown by the $O_{ph}-Mn-O_{ac}$ angles of 92.00(9)° and 98.27(9)° made by one acetate bridge at Mn(1) and Mn(2), respectively. Also, while both Mn(II) ions are drawn slightly toward the phenoxo oxygen out of the respective N_2O_2 planes perpendicular to the $Mn-O_{ph}$ vectors, the displacement of Mn(2) is longer (0.124(2) Å) than that of Mn(1) (0.073(2) Å). The intramolecular Mn−Mn distance of 3.469(2) Å is close to that in **2** but smaller than thatin **3** (Table 4), and all three are within the range of about 3.3−3.7 Å observed in μ-O_{H_2O}-bis-carboxylato[17,36] and μ-O_{ph}-bis-μ-carboxylato[26a,d,37] dinuclear Mn(II) complexes. The $Mn-O_{ac}$, $Mn-N_{am}$, and $Mn-N_{py}$ distances in **1** are also in the range commonly observed in analogous Mn(II) complexes.[20a,21,26,37−40]

Table 4. Selected Bond Distances (Å) of Relevant Mn_2(II,II) and Mn_2(II,III) Complexes

	2[27]	**2ox**[20]	**1**[a]	**1ox**[a]	**3**[21]
Mn−Mn	3.412(1)	3.447(1)	3.469(3)	3.486(6)	3.547(6)
Mn(II)−O_{ph}[b]	2.117(3)	2.193(4)	2.133(2)	2.237(6)	2.125(3)
	2.103(3)		2.113(2)		2.140(3)
Mn(III)−O_{ph}		1.903(4)		1.891(6)	
Mn(II)−N_{am}	2.320(4)	2.324(5)	2.352(3)	2.341(5)	2.301(2)
	2.331(4)		2.354(6)		2.309(2)
Mn(III)−N_{am}		2.073(5)		2.065(5)	
Mn(II)−N_{py}	2.311(4)$_{cis}$[c]	2.271(6)$_{cis}$	2.301(3)$_{cis}$	2.247(5)$_{cis}$	2.358(1)$_{cis}$
	2.295(4)$_{cis}$	2.210(6)$_{tr}$	2.302(5)$_{cis}$	2.228(6)$_{tr}$	2.335(3)$_{cis}$
	2.298(4)$_{tr}$		2.298(3)$_{tr}$		2.324(1)$_{tr}$
	2.267(4)$_{tr}$		2.341(2)$_{tr}$		2.314(7)$_{tr}$
Mn(III)−N_{py}		2.235(6)$_{cis}$		2.290(7)$_{cis}$	
		2.052(5)$_{tr}$		2.035(7) $_{tr}$	
$C_{ph}-O_{ph}$	1.339(6)	1.364(7)	1.344(3)	1.376(4)	1.3507(6)

changes in bond lengths on oxidation

$\delta[C_{ph}-O_{ph}]$	**2** → **2ox** = +0.025	**1** → **1ox** = +0.032
δ[Mn(II)−O_{ph}]	**2** → **2ox** = +0.083	**1** → **1ox** = +0.113
δ[Mn(II)−$N_{py,tr}$]	**2** → **2ox** = −0.073	**1** → **1ox** = −0.092
δ[Mn(II)−$N_{py,cis}$]	**2** → **2ox** = −0.022	**1** → **1ox** = −0.054

average coordination bond lengths:

	2[27]	**2ox**[20]	**1**[a]	**1ox**[a]	**3**[21]
Mn(II)	2.212	2.205	2.227	2.212	2.239
Mn(III)		2.047		2.059	

decrease in the average coordination bond length (Å) on oxidation

Mn(II) in **2** → Mn(III) in **2ox** = − 0.165	Mn(II) in **1** → Mn(III) in **1ox** = − 0.165

[a] This work. [b] ph = phenolate; py = pyridyl; am = amine. [c] cis and tr refer to cis and trans coordination to the bridging phenoxo oxygen.

Structure of $[Mn_2(L^1O)(\mu\text{-}OAC)_2](ClO_4)_2\cdot 2CH_2Cl_2$, (1ox)·2($CH_2Cl_2$). X-ray diffraction quality crystals of **1ox**, obtained in high yield from CH_2Cl_2 solutions layered with $(C_2H_5)_2O$, are formed with two molecules of CH_2Cl_2 as solvent of crystallization.

However, when the mixture stands at room temperature, these solvent molecules are readily lost, hence the elemental analysis best fits the formula $[Mn_2L^1O(OAc)_2](ClO_4)_2$. X-ray data collection was therefore performed at 103(2) K on freshly harvested crystals.[41] Figure 3 shows an ORTEP diagram of the cation of **1ox**, $[Mn_2(L^1O)(\mu\text{-}OAc)_2]^{2+}$. The crystal data and refinement parameters and selected bond lengths and angles in **1ox** are shown in Tables 1 and 3, respectively. Complex **1ox** is a dinuclear mixed-valent complex in which the Mn(II) and Mn(III) ions, bridged by the phenoxo oxygen and two acetates and separated by 3.486(6) Å, are each in a distorted octahedral environment**.** The three nitrogens of each of the two chelating arms coordinate

(36) (a) Caneschi, A.; Ferraro, F.; Gatteschi, D.; Melandri, M. C.; Rey, P.; Sessoli, R. *Angew. Chem., Int. Ed. Engl.* **1989**, *28*, 1365. (b) Howard, T.; Tesler, J.; DeRose, V. J. *Inorg. Chem.* **2000**, *39*, 3379.
(37) Mikuriya, M.; Fujii, T.; Kamisawa, S.; Kawasaki, Y.; Tokii, T.; Oshio, H. *Chem. Lett.* **1990**, 1181.
(38) Fraser, C.; Johnston, L.; Rheingold, A. L.; Haggerty, B. S.; Williams, G. K.; Whelan, J.; Bosnich, B. *Inorg. Chem.* **1992**, *31*, 1835.
(39) Hodgson, D. J.; Schwarts, B. J.; Sorrell, T. N. *Inorg. Chem.* **1989**, *28*, 2226.
(40) Sakiyama, M.; Tamaki, H.; Kodera, M.; Matsumoto, N.; Okawa, H. *J. Chem. Soc., Dalton, Trans.* **1993**, 591.
(41) There was one ordered and one badly disordered CH_2Cl_2 molecule. The latter was handled by the subroutine squeeze in PLATON (Spek, A. L. *J. Appl. Cryst.* **2003**, *36*, 7−13), which removes the contribution of the disordered part, then calculates the void volume and integrates over this volume to find the number of electrons. This results in 72 electrons per unit cell or 36 electrons per asymmetric unit and a void volume of 328.5 Å^3. Because a full CH_2Cl_2 group has 42 electrons, this means that the disordered CH_2Cl_2 has occupancy of 0.857.

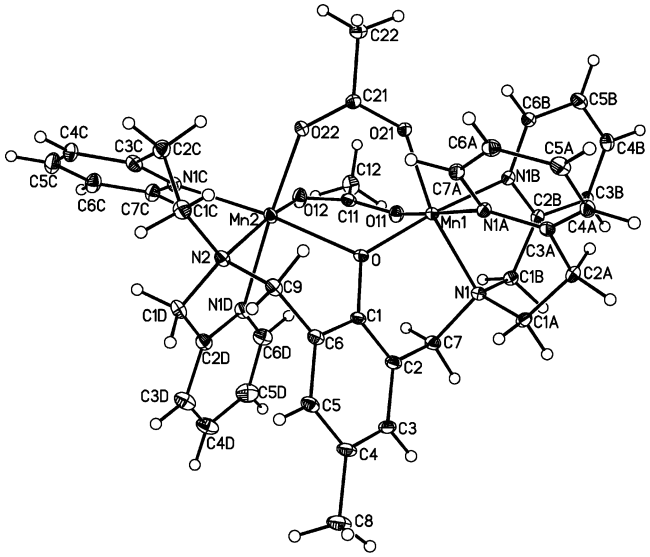

Figure 3. ORTEP diagram showing the labels and the 20% probability ellipsoids of the positions of the atoms in the structure of the cation of **1ox**.

facially, forming one five- and one six-membered chelate ring. The two manganese ions, Mn(1) in the +3 oxidation state and Mn(2) in the +2 oxidation state, have distinctly different coordination bond distances and angles. Four of the six bonds to Mn(1) are distinctly shorter than the two trans-axially coordinating donors (which are Jahn−Teller elongated) and are also shorter than the corresponding bonds of Mn(2). The Jahn−Teller effect makes the axial position in Mn(1) (cis to the phenoxo oxygen) preferable for coordination by N_{py} with the longer 2-(2-pyridyl)ethyl arm, while in Mn(2), this donor group is coordinated trans to the phenoxo oxygen, making the structure of this complex unsymmetrical with respect to the manganese coordination environments.

Tables 4 and 5 show the coordination bonding parameters of **1**, **1ox**, and a set of analogous complexes. The Mn−Mn distances and Mn−O_{ph}−Mn angles of **1** and **1ox** lie in the range of about 3.3−3.7 Å and 107−117°, respectively, as observed in other similar Mn_2(II,II), Mn_2(II,III) bis-1,3-μ-carboxylato complexes with additional bridging by a phenoxo oxygen, H_2O, or OH^-.[37,42,43,44] Upon oxidation of **1** to **1ox**, the Mn−O−Mn angle and the Mn−Mn distance increase, as observed in other analogous complexes (Table 4).[20,26a,27] In addition, the sum of the three bond angles of the phenoxo oxygen decreases by 2.1° consistent with similar changes found in the structural data of **2**[27] and **2ox** [20] (see Table 5) indicating that oxidation is accompanied by some loss in planarity in the bonding at the bridging phenoxo oxygen. There is also an increase in the Mn(II)−O_{ph}−C_{ph} bond lengths and a decrease in the Mn(II)−N_{py} bond lengths, while in contrast, there are no significant changes in the Mn(II)−N_{am} bond lengths (Table 4) upon oxidation. These simultaneous changes in planarity and bond lengths are strongly suggestive of a C_{ph}−O_{ph}−Mn(II)−N_{py} extended π-bonding system in these complexes. The C_{ph}−O_{ph}−Mn(II) π-chain is weakened in favor of strengthening the Mn(II)−N_{py} bonds upon oxidation of one of the two Mn(II) ions to Mn(III). The weakening of the Mn(II)−O_{ph}−C_{ph} bond is likely to be caused by the withdrawal of electron density from the C_{ph}−O_{ph}−Mn(II) extended π-bonding system by Mn(III) (which may itself have π-overlap with O_{ph}), which in turn, enhances the N_{py}-to-Mn(II) π-donation and thereby shortens those bonds. A similar finding is that the analogous Mn_2(II,II) complex of L^2OH bearing an electron-withdrawing NO_2 para substituent on the phenoxo ring shows a longer Mn−O_{ph} bond and a shorter C−O_{ph} bond than those in **2**,[45] consistent with the notion of electron withdrawal from the Mn−O_{ph} bond through the π-bond system. The involvement of metal−pyridyl π-bonding in manganese [21,45] and iron complexes[46a,b] and in Mn−O−Mn bridging bonds[46c] has been demonstrated.

Among these O_{ph}- and bis-acetato-bridged dinuclear manganese complexes, the Mn_2(III,III) state of the L^1OH and L^2OH complexes is not known, while only the Mn_2(II,II) complex and no higher oxidation state complexes of L^3OH are known in the stable state (electrochemistry section). As evidence that the Mn_2(III,III) complexes are unstable, the

Table 5. Selected Bond Angles (deg) of Relevant Mn_2(II) and Mn_2(II,III) Complexes

	2[27]	**2ox**[20a]	**1**[a]	**1ox**[a]	**3**[21,28]
Mn−O_{ph}−Mn	107.9(1)	114.4(2)	109.54(9)	115.0(2)	112.50(9)
Mn(II)−O_{ph}−C_{ph}[b]	126.7(3)	121.0(3)	120.44(17)	114.73	123.57(9)
	125.2(3)		128.26(18)		123.88(9)
Mn(III)−O_{ph}−C_{ph}		123.7(3)		126.40(16)	
O_{ph}−Mn(II)−$N_{py(tr)}$[b,c]	158.52(15)	156.4(2)	165.50(9)	167.78(7)	172.58(1)
			170.42(10)		174.090(8)
Oph−Mn(III)−$N_{py(tr)}$		170.2(2)		174.17(8)	

sum of bond angles at O_{ph}

2[27]	**2ox**[20a]	**1**[a]	**1ox**[a]	**3**[21,28]
359.8	359.1	358.2	356.1	360.0

change in the sum of bond angles at O_{ph} on oxidation

2 → **2ox** = −0.7 **1** → **1ox** = −2.1

average chelate angle at Mn(II)

2[27]	**2ox**[20a]	**1**[a]	**1ox**[a]	**3**[21,28]
74.15	74.8	77.61	78.35	84.97(5)
73.67	81.25	84.88(7)		

average chelate angle at Mn(III)

2ox[20a]	**1ox**[a]
79.3	84.76

[a] This work. [b] ph = phenoxo; py = pyridyl. [c] cis and tr refer to cis and trans coordinations to the bridging phenoxo oxygen.

(42) (a) Romero, I.; Collomb, M.-N.; Llobet, A.; Perret, E.; Pécaut, J.; Lepape, L.; Latour, J.-M. *Eur. J. Inorg. Chem.* **2001**, 69. (b) Pal, S.; Olmstead, M. M.; Armstrong, W. H. *Inorg. Chem.* **1995**, *34*, 4708. (c) Mok, H. J.; Davis, J. A.; Pal, S.; Mandal, S. K.; Armstrong, W. H. *Inorg. Chim. Acta* **1997**, *263*, 385.

(43) Higuchi, C.; Sakiyam, H.; Okawa, H.; Fenton, D. J. *J. Chem. Soc., Dalton Trans.* **1995**, 4015.

(44) Yamami, M.; Tanaka, M.; Sakiyama, H.; Koga, T.; Kobayashi, K.; Miyasaka, H.; Ohba, M.; Okawa, H. *J. Chem. Soc., Dalton Trans.* **1997**, 4595.

(45) Blanchard, S.; Blain, G.; Riviere, E.; Nierlich, M.; Blondin, G. *Chem.—Eur. J.* **2003**, *9*, 4260.

(46) (a) Jones, C. M.; Johnson, C. R.; Asher, S. A.; Shepard, R. E. *J. Am. Chem. Soc.* **1985**, *107*, 3772. (b) Johnson, C. A.; Shepard, R. E. *Inorg. Chem.* **1983**, *22*, 3506. (c) Brunold, T. C.; Gamelin, D. R.; Solomon, E. I. *J. Am. Chem. Soc.* **2000**, *122*, 8511.

reactions of L^1OH,[47] L^2OH,[20] and similar dinucleating ligands[26] with $Mn(III)(OAc)_3 \cdot 4H_2O$ only yield stable complexes in the $Mn_2(II,III)$ state (**1ox**, **2ox**) and none in the $Mn_2(III,III)$ state. These instabilities are rationalized by the difference in the coordination geometry and radii requirements of the Mn(II) and Mn(III) ions. In octahedral fields, while the high-spin d^5 Mn(II) (radius 1.0 Å)[48] adopts bond lengths and angles that are sterically imposed by the ligand, the smaller d^4 Mn(III) ion (radius 0.79 Å) is stabilized by shorter bond distances and Jahn−Teller distorted but regular octahedral angle geometry. Thus the steric properties (such as the chelate arm length) of the ligand dictate the coordination sphere radii and geometry and can be the dominant factors in determining the thermodynamically stable and isolable oxidation states of these metal complexes. Chelating ligands that preclude short bonds or impose rigid distortion to the octahedral geometry angles, because of overly high chelate ring strains, destabilize the Mn(III) state with respect to reduction Mn(II).[39,49]

Among the present complexes, the average coordination sphere radii[50] increase with an increase in the chelate ring sizes of the ligands in the order **2** < **1** < **3**, as demonstrated by the following coordination sphere radii in the present set of complexes: Mn(II) sites **2** (2.212 Å) < **1** (2.227 Å) < **3** (2.237 Å), **2ox** (2.205 Å) < **1ox** (2.212 Å); Mn(III) sites **2ox** (2.041 Å) < **1ox** (2.059 Å) (Table 4). The cyclic voltammetric potentials (electrochemistry section below) increase with the increasing average coordination radii.

Upon the one-electron oxidation of **1,** there is a net decrease of 0.165 Å from the average coordination radius of Mn(II) in **1** to that of Mn(III) in **1ox**. There are also important changes in the coordination of the Mn(II) ion **1ox** from that in **1**, including an increase in the $Mn(II)-O_{ph}$ bond length by 0.114 Å and decreases in the $Mn(II)-N_{py,tr}$ and $Mn(II)-N_{py,cis}$ bond lengths (by 0.093 and 0.054 Å respectively). Although, after these changes, the net average coordination radius of Mn(II) in **1ox** remains practically unchanged from that in **1**, the changes have significance in that they result in coordination about the Mn(II) ion in **1ox**, losing its flexibility to reduce its radius enough (without increasing chelate angle strain) to stabilize Mn(III) in a second-electron oxidation of the complex. Thus the Mn_2-(III,III) complex, when formed, is unstable with respect to reduction back to the Mn_2(II,III) state (see below in the electrochemistry section).

The same structural changes also occur in the oxidation of **2** to **2ox**, albeit on a smaller scale (Table 4), but in this case, they are accompanied by a significant increase in the degree of distortion of the octahedral geometry (measured by the sum of the absolute deviations of the cis angles of coordination from 90°)[51,52] at the Mn(II) ion in **2ox,** which makes the site unsuitable for coordination of Mn(III). Thus, Mn_2(III,III) cannot be isolated.

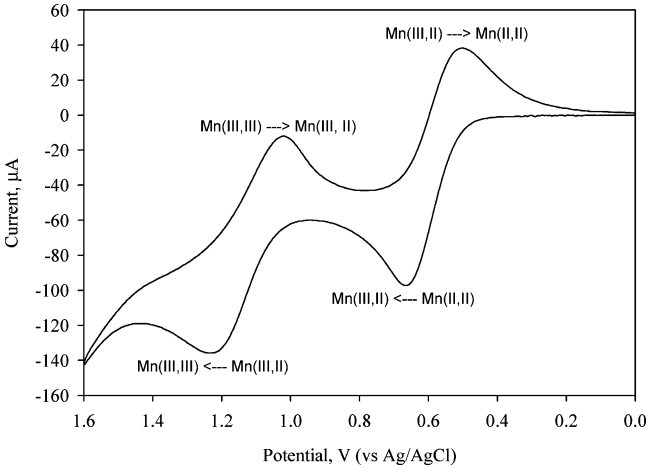

Figure 4. Cyclic voltammogram of $[Mn(II)_2(LO)(CH_3COO)_2]ClO_4$ (**1**) in acetonitrile solution (2.0 mM) showing two quasi-reversible redox processes (glassy carbon working, Ag/AgCl reference, and Pt wire counter electrodes, 0.1 M $(n\text{-}Bu)_4NClO_4$ supporting electrolyte at 100 mV/s).

Table 6. Cyclic Voltammetric Potentials of **1** and Analogous Complexes[c]

	redox potentials (V vs Ag/AgCl)		
	$Mn_2(II,II) \leftrightarrow Mn_2(II,III)$	$Mn_2(II,III) \leftrightarrow Mn_2(III,III)$	ref
1	$E_{1/2} = 0.59$ (q-rev)[a]	$E_{pc} = 1.20$ (irrev)	this work
2	$E_{1/2} = 0.47$ (q-rev)[b]	$E_{1/2} = 1.13$ (q-rev)	20a,b
	$E_{1/2} = 0.47$ (q-rev)[b]	$E_{1/2} = 1.02$ (q-rev)	20c
3	$E_{1/2} = 0.65$ (q-rev)[a]	$E_{pc} = 1.22$ (irrev)	28
4	$E_{1/2} = 0.73$ (q-rev)[a]	$E_{pc} = 1.28$ (irrev.)	21
5	$E_{1/2} = 0.435$ (q-rev)	$E_{1/2} = 1.01$ (q-rev)	12h

[a] Versus Ag/AgCl in acetonitrile.
‡ Versus SCE (in acetonitrile). [c] **1** = $[Mn_2(L^1O)(\mu\text{-}OOCCH_3)_2]ClO_4$; **2** = $[Mn_2(L^2O)(\mu\text{-}OOCCH_3)_2](ClO_4)_2 \cdot H_2O$; **3** = $[Mn_2(L^3O)(\mu\text{-}OOCCH_3)_2]ClO_4$, LOH = 2,6-bis(bis-(2-pyridyl)ethyl)aminomethyl-4-methylphenol; **4** = $[Mn_2(LO)(\mu\text{-}OOCCH_3)_2]ClO_4$, LOH = 2,6-bis(bis-(2-pyridyl)ethyl)aminomethyl-phenol; **5** = $[Mn_2(L\text{-}Im)(\mu\text{-}OOCCH_3)_2](ClO_4)_2$ (L-Im) = 2,6-bis-{bis(1-methylimidazolyl)methyl)aminomethyl}-4-methylphenol.

Electrochemistry. The cyclic voltammogram of **1** in CH_3-CN is shown in Figure 4. Two quasi-reversible redox processes are observed at potentials (vs Ag/AgCl) $E_{1/2}$ = 0.59 V (ΔE_p = 190 mV) and at $E_{1/2}$ = 1.18 V (ΔE_p = 260 mV). These are assigned to the $Mn_2(II,II) \leftrightarrow Mn_2(II,III)$ and $Mn_2(II,III) \leftrightarrow Mn_2(III,III)$ redox processes, respectively. Table 6 summarizes the cyclic voltammetric redox potentials of **1** and the analogous manganese complexes **2**−**5**. The potential for the $Mn_2(II,II) \leftrightarrow Mn_2(II,III)$ redox process of **1** (0.59 V) is approximately the mean of the corresponding potentials of **2** and **3** and consistent with the trend of increasing chelate ring sizes**.** The oxidation potentials increase with increasing chelate ring sizes[53,54] because of the attendant increase in the coordination sphere radii and the

(47) From the reaction of L^1OH with $Mn(OAc)_3 \cdot 4H_2O$, CH_3COONa, and NEt_3 in CH_3CN, we isolated a brown powdery solid which showed the same absorption spectrum as **1ox**, consistent with the observations by others on the identical reaction with L^2OH (ref 20) and a closely similar ligand (ref 25a).
(48) (a) Shannon, R. D. *Acta Crystallogr.* **1976**, *A32*, 751. (b) Sakiyama, H.; Sugawara, A.; Sakamoto, M.; Unuora, K.; Inoue, K.; Yamasaki, M. *Inorg. Chim. Acta* **2000**, *310*, 163.
(49) Drew, M. G. B.; Harding, C. J.; McKee, V.; Morgan, G. G.; Nelson, J. *J. Chem. Soc. Chem. Commun.* **1995**, 1035.
(50) The average coordination sphere radius is taken as the average coordination bond length.
(51) (a) McCrea, J.; McKee, V.; Metcalfe, T.; Tandon, S.; Wikaira, J. *Inorg. Chim. Acta* **2000**, *297*, 220. (b) Milios, C. J.; Raptopoulou, C. P.; Terzis, A.; Vicente, R.; Escuer, A.; Perlepes *Inorg. Chem. Commun.* **2003**, *6*, 1056.
(52) Tandon, S. S,; Chander, S.; Thompson, L. K. *Inorg. Chim. Acta* **2000,** *300*, 683.

resulting decrease in stability of the Mn(III) ion to reduction. Thus while **1** and **2** can be oxidized to stable Mn_2(II,III) states (**1ox** and **2ox**, respectively), only the Mn_2(II,II) state of **3** is known to be stable. The redox potentials of **3** are significantly lower than those of **4** (Table 6) showing the electronic inductive effect of the methyl group para to the bridging phenoxo oxygen.

The size of the difference between the $E_{1/2}$ values of the two electrochemically reversible redox processes in the cyclic voltammetry ($\Delta E_{1/2}$) of a dinuclear metal complex is an indicator of the relative stability of the mixed-valent state to disproportionation (K_{com})

$$Mn_2(II,II) + Mn_2(III,III) \leftrightarrow 2Mn_2(II,III)$$

The redox processes here are not ideally reversible, so that the values of $\Delta E_{1/2}$ (0.66, 0.61, and 0.55 V for **2**, **1**, and **3)** give only approximate values of the comproportionation constants, K_{com} (given by $\Delta E_{1/2} = (RT/nF) \log K_{com}$), as 1.55 $\times$ 10^{11}, 2.18 $\times$ 10^{10}, and 2.10 $\times$ 10^9. The large $\Delta E_{1/2}$ (large K_{com}) values indicate that the Mn(II,II) and the Mn(III,III) states readily comproportionate to the more stable mixed-valent Mn_2(II,III) state. In such complexes, stepwise one-electron processes take place at widely different potentials. Dinuclear Mn(II) complexes in which the two metal ions, in equivalent coordination states, are electronically insulated from each other by the bridging group[15a,b,16b] exhibit zero or small $\Delta E_{1/2}$ values and undergo two-electron redox processes at the same potential[13a−c] In such cases, the Mn(II,III) states are unstable to disproportionation. In the present set of complexes, the structural changes from the first electron oxidations of **1** and **2** elevate the potential of the second electron oxidation leading to a large $\Delta E_{1/2}$.

Controlled Potential Electrolysis. The controlled potential electrolytic oxidation of 5.2 $\times$ 10^{-5} mol of **1** at 0.7 V vs Ag/AgCl requires a total charge of 4.7 $\times$ 10^{-5} F, which corresponds to a one-electron oxidation of **1**. The colorless binuclear Mn(II,II) complex becomes green in a few minutes, and at the end of the electrolysis, the solution becomes dark green. Electrolytic reduction of the green solution at 0.2 V (vs Ag/AgCl) restores the colorless solution, which also takes up one electron per dinuclear complex as shown by coulometric measurements. Electrolysis of the colorless solution at 0.7 V regenerates the green solution. After 8 such oxidation−reduction electrolytic cycles, about a 5% loss of the complex was observed judging both by coulometric and electronic absorption measurements. Complexes **1** and **1ox** could be isolated from the solution at the end of the respective half-cycles.

The electrolytic oxidation of **1ox** in acetonitrile at a potential of 1.2 V (vs Ag/AgCl) takes up slightly greater than 1.0 F/mol, but **1ox** is the major isolated product after electrolysis showing that the Mn_2(III,III) state is formed and that it is reduced back to the stable Mn(II,III) state. The visible electronic absorption spectrum of the green solution after electrolysis showed decreased absorbance compared to the starting solution, which likely the result of some ligand decomposition. The electrolytic oxidation of **3** at 0.8 V (vs Ag/AgCl in acetonitrile also took 1 F/mol of complex to yield a brown solution which shows an absorption spectrum in the visible region similar to that of **1ox**. However, upon standing, the brown solution fades away to yield a pale yellow solution, showing the instability of the Mn(II,III) state to reduction back to the Mn(II,II) state.[28]

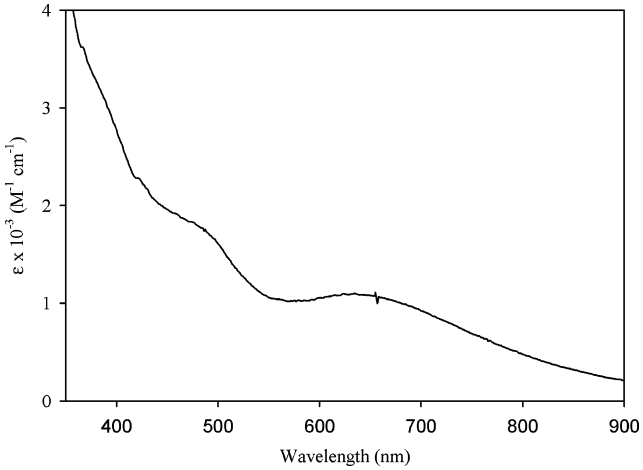

Figure 5. The electronic absorption spectrum of **1ox** in acetonitrile solution.

Electronic Absorption Spectrum. Complex **1** shows absorption in the UV region resulting from pyridyl intraligand electronic transitions at 257 (ϵ = 1.36 $\times$ 10^4 M^{-1} cm^{-1}) and 311 nm (ϵ = 3.55 $\times$ 10^3 M^{-1} cm^{-1}) and no d−d absorption in the visible region, as expected for high-spin d^5 ion in octahedral coordination. An acetonitrile solution of **1ox** shows strong absorbance peaks in the visible region (Figure 5) at λ_{max} = 410 nm (shoulder, ϵ = 2.3 $\times$ 10^3 M^{-1} cm^{-1}) assigned to a phenoxo-oxygen-to-Mn(III) charge-transfer transition and at 486 (ϵ = 1.7 $\times$ 10^3 M^{-1} cm^{-1}) and 645 nm (ϵ = 1.1 $\times$ 10^3 M^{-1} cm^{-1}) assigned as ligand field transitions, in accordance with assignments of similar peaks in the spectra of **2ox** (λ_{max} = 480 and ~620 nm)[20] and other analogous complexes.[26] The longer λ_{max} of the ligand field absorptions of **1ox** relative to the equivalent absorptions of **2ox** are in keeping with the expected weaker ligand field in **1ox** attributable to the longer average Mn(III) coordination radius.[54]

Infrared Absorption Spectra. The infrared spectra of both **1** and **1ox** in Nujol show absorption peaks at 1580 and 1420 cm^{-1}, as expected because of the asymmetric and symmetric stretching vibrations, respectively, of the 1,3-bridging acetate ligand. The difference in the frequencies of the two absorption peaks ($\Delta\nu$) of 160 cm^{-1} is diagnostic of 1,3-bridging carboxylato.[55] Strong absorption peaks at 1600 cm^{-1} from the pyridyl ring and at 1110 cm^{-1} from ClO_4^- are also observed.

(53) Zubieta, J.; Karlin, K. D.; Hayes, J. C. *Copper Coordination Chemistry, Biochemical and Inorganic Perspectives*; Karlin, K. D., Zubieta, J., Eds.; Adenine Press: Albany, NY, 1983; p 97.
(54) Zhang, D.; Busch, D. H. *Inorg. Chem*. **1994**, *33*, 5138.
(55) Nakamoto, K. *Infrared and Raman Spectra of Inorganic and Coordination Compounds*, 5th ed.; Wiley-Interscience: New York, 1997; Part B, p 60.

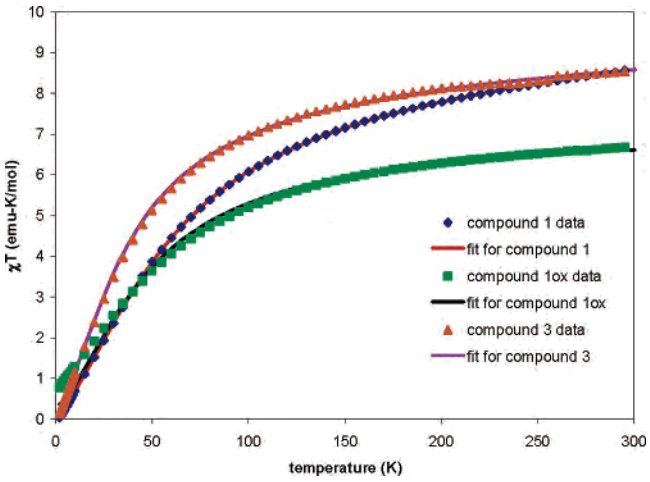

Figure 6. Plot showing the dependence of χT (the product of the molar magnetic susceptibility and the temperature) of **1**, **1ox**, and **3** on temperature. The solid lines result from a least-squares fit of the data to the theoretical equations shown above.

Magnetic Properties. The temperature-dependent magnetic data for the Mn_2(II,II) complexes **1** and **3** were modeled using a Heisenberg Hamiltonian of the form $H = -2J\hat{S}_iS_j$ which was used in studies of similar Mn_2(II,II) and Mn_2(II,III) dimanganese complexes.[26a] The equation below was used to model the Mn_2 (II,II) data

$$\chi_m T = \frac{2N_A g^2 \beta^2}{4k_B} \frac{\exp(2x) + 5\exp(6x) + 14\exp(12x) + 30\exp(20x) + 55\exp(30x)}{1 + 3\exp(2x) + 5\exp(6x) + 7\exp(12x) + 9\exp(20x) + 11\exp(30x)} + aT$$

For the corresponding (II,III) dinuclear species, the model is given by

$$\chi_m T = \frac{N_A g^2 \beta^2}{4k_B} \frac{1 + 10\exp(3x) + 35\exp(8x) + 84\exp(15x) + 165\exp(24x)}{1 + 2\exp(3x) + 3\exp(8x) + 4\exp(15x) + 5\exp(24x)}$$

where χ_m is the magnetic susceptibility, $x = \exp(-J/kT)$, N_A is the Avogadro number, g is the Zeeman splitting factor, β is the Bohr magneton, J is the coupling constant, k_B is Boltzmann's constant, T is the absolute temperature, a is the temperature independent paramagnetism term, and everything else has its usual meaning. The data and fit for the complexes **1**, **1ox**, and **3** are shown in Figure 6. The best least-squares fit of the experimental data were obtained when $g = 2.00 \pm 0.01$ and $J = -4.3 \pm 0.1$ cm^{-1} for **1** and $g = 2.00 \pm 0.01$ and $J = -2.7 \pm 0.1$ cm^{-1} for **3**, which indicate weak antiferromagnetic coupling in each complex. The quality of the fit is excellent, which is to be expected considering that the spin state of Mn(II) is isotropic $S = 5/2$, with no orbital contribution, for which the model should work well.

However in the case of **1ox**, a fit as good as those of **1** and **3** could not be obtained, probably indicating zero-field splitting of the Mn(III) state on the order of the coupling constant (J) that is not accounted for. The best least-squares fit for the experimental data of $\chi_m T$ vs T, obtained for $g = 2.00$, was determined with $J = -4.1 \pm 0.1$ cm^{-1}, which is close to that obtained for **1** and in the range exhibited by similar Mn_2(II,III) complexes.[26,56]

The decreasing order of the magnitude of the J values of the three Mn_2(II,II) complexes, **2**, **1**, and **3**, (-4.8,[27] -4.3, and -2.7 cm^{-1}, respectively) parallels the increasing order of Mn−Mn distances, the average Mn(II)-O_{ph} bond distances, and the Mn−O_{ph}−Mn bridge angles[17d,23] (Table 4). Dubois et al.[26a] have observed that among μ-carboxylato-μ-O_{ph} Mn(II,II) complexes with similar Mn−O−Mn angles, there is an approximate linear relationship between the values of J and the Mn−O_{ph} distances, showing that the value of J is dependent on both the bridge angle and bond distances,[26a,45] two factors that determine the degree of orbital overlap responsible for magnetic coupling between the metal ions. Complex **1ox** exhibits a smaller J value (-4.1 cm^{-1}) than **2ox** (-6.0 cm^{-1}),[20b] consistent with its longer Mn−Mn distance and Mn(II)−O_{ph} bond lengths but similar Mn−O_{ph}−Mn bridge angles and with the trend observed among Mn_2(II,III) complexes of increasing magnitude of J with a decrease in the difference between the bridge bond distances Mn(II)−O_{ph} and Mn(III)−O_{ph}.[26a] The complexes studied here are among the Mn_2(II,II) and Mn_2(II,III) complexes in the literature with 1,3-μ-carboxylato and O_{ph}, H_2O, or OH^- bridging which show generally weak antiferromagnetic coupling.[9a,36a,37,57−59]

Conclusion

Using the dinucleating ligand 2,6-bis[(2-(2-pyridyl)ethyl)-(2-pyridylmethyl)-aminomethyl]-4-methylphenol) (L^1OH)) which bears two arms each with a donor set forming one five- and one six-membered chelate ring, we have synthesized and structurally, electrochemically, and spectroscopically characterized the stable discrete dinuclear Mn_2(II,II) complex, $[Mn_2(L^1O)(\mu\text{-}OAc)_2](ClO_4)$ (**1**), and its Mn_2(II,III) oxidation product, $[Mn_2(L^1O)(\mu\text{-}OAc)_2\}(ClO_4)_2$ (**1ox**). The Mn_2(II,II) and Mn_2(II,III) states are interconvertible for several cycles by electrolytic oxidation and reduction at 0.7 and 0.2 V vs Ag/AgCl, respectively, at a platinum electrode. The cyclic voltammetric potentials for the Mn_2(II,II) ↔ Mn_2(II,III) and Mn_2(II,III) ↔ Mn_2(III,III) redox process are intermediate between the corresponding potentials of the analogous complexes of the ligands 2,6-bis (bis (2-pyridylmethyl)-aminomethyl]-4-methylphenol) (L^2OH), which forms

(56) (a) Baskin, J. S.; Schake, A. R.; Vincent, J. B.; Huffman, J. C.; Christou, G.; Chang, H.-R.; Li, Q.; Hendrickson, D. N. *J. Chem. Soc., Chem. Commun.* **1988,** 700. (b) Chang, H.-R.; Larsen, S.; Pierpont, C. G.; Boyd, P. D. W.; Hendrickson, D. N. *J. Am. Chem. Soc.* **1988**, *110*, 4565. (c) Dismukes, G. C.; Sheats, J. E.; Smegal, J. A. *J. Am. Chem. Soc.* **1987**, *109*, 7202.
(57) (a) Higuchi, C.; Sakiyama, H.; Okawa, H.; Isobe, R.; Fenton, D. E. *J. Chem. Soc., Dalton Trans*. **1994**, 1097. (b) Aono, T.; Wada, H.; Yonemura, M.; Okawa, H.; Fenton, D. E. *J. Chem. Soc., Dalton Trans*. **1997**, 1527.
(58) Bossek, U.; Wieghardt, K. *Inorg. Chim. Acta* **1989**, *165*, 123.
(59) (a) Baldwin, M. J.; Kampf, J. W.; Kirk, M. I.; Pecoraro, V. I. *Inorg. Chem.* **1995**, *34*, 5252. (b) Takanori, A.; Wada, H.; Yonemura, M.; Ohba, M.; Okawa, H.; Fenton, D. E. *J. Chem. Soc., Dalton Trans.* **1997**, 1527.

all five-membered chelate rings, and 2,6-bis-(bis-(2-(2-pyridyl)ethyl)-aminomethyl)-4-methylphenol)(L^3OH), which forms all six-membered chelates. The changes in bond angles and lengths observed upon oxidation of **1** and **2** are consistent with the presence of a π-bond system extended over the phenoxo aromatic system $C_{ph}-O_{ph}-Mn(II)-N_{py}$ chain. We have shown, for these dinuclear complexes, that the structural changes that occur at one metal site with the first electron oxidation are transmitted via the bridging group to the coordination site of the second metal ion, changing the coordination geometry, and consequently destabilizing the Mn(III,III) state to reduction to the Mn(II,III) state. The mixed-valent states (Mn(II,III) and Mn(III,IV)) of manganese catalases, formed by one-electron redox reactions of the active (Mn(II,II) and Mn(III,III) forms, are catalytically inactive hence the mechanism of suppression of their formations may be crucial in high efficiency enzymatic catalase activity. **1** and **1ox** show weak antiferromagnetic coupling with J in the range from -3 to -10 cm^{-1}, as Mn_2-(II, III) complexes of this type generally do. The magnitude of the J values of the Mn_2(II,II) complexes **1**, **2**, and *3* decrease with increasing Mn−Mn and $Mn-O_{ph}$ bond distances and $Mn-O_{ph}-Mn$ angles, consistent with the order of decrease in the degree of orbital overlap. The Mn_2(II,III) complexes **1ox** and **2ox** show the same general trends in their values of J and additionally fit in the general trend shown by the analogous complexes, that the magnitude of J increases with decrease in the difference between the Mn-(II)$-O_{ph}$ and Mn(III)$-O_{ph}$ bond lengths.

Acknowledgment. Y.G. would like to thank the NIH and EPA GEM programs for partial graduate student financial support and the Provost's Office of Howard University for support for supplies. R.J.B. would like to acknowledge funding by the U. S. DoD for upgrading of our diffractometer. G.T.Y. thanks the NSF and the Virginia Tech ASPIRES program for each providing partial funding for the purchase of the SQUID.

Supporting Information Available: Details of crystallographic structural information in CIF format. This material is available free of charge via the Internet at http://pubs.acs.org.

IC060039Q